Biochimica et Biophysica Acta 1787 (2009) 234–241

Contents lists available at ScienceDirect

Biochimica et Biophysica Acta

journal homepage: www.elsevier.com/locate/bbabio

# Characterisation of the electron transfer and complex formation between Flavodoxin from *D. vulgaris* and the haem domain of Cytochrome P450 BM3 from *B. megaterium*

Andrea Fantuzzi [a], Yergalem T. Meharenna [a,b], Paul B. Briscoe [a], Francoise Guerlesquin [c], Sheila J. Sadeghi [a,d], Gianfranco Gilardi [a,d,*]

[a] *Division of Biomolecular Sciences, Imperial College London, SW7 2AZ London, UK*
[b] *Department of Molecular Biology and Biochemistry, University of California, Irvine, CA, USA*
[c] *Unité Interactions et Modulateurs de Réponses, CNRS Marseille, France*
[d] *Department of Human and Animal Biology, University of Turin, Turin, Italy*

ARTICLE INFO

*Article history:*
Received 21 August 2008
Received in revised form 9 January 2009
Accepted 13 January 2009
Available online 30 January 2009

*Keywords:*
Electron transfer
Flavodoxin
P450 BMP
Transient complex
Protein–protein docking

ABSTRACT

Investigation of the complex formation and electron transfer kinetics between P450 BMP and flavodoxin was carried out following the suggested involvement of flavodoxin in modulating the electron transfer to BMP in artificial redox chains bound to an electrode surface. While electron transfer measurements show the formation of a tightly bound complex, the NMR data indicate the formation of shortly lived complexes. The measured $k_{obs}$ ranged from 24.2 $s^{-1}$ to 44.1 $s^{-1}$ with $k_{on}$ ranging from $0.07\times10^6$ to $1.1\times10^6$ $s^{-1}M^{-1}$ and $K_d$ ranging from 300 μM to 24 μM in buffers of different ionic strength. This apparent contradiction is due to the existence of two events in the complex formation prior to electron transfer. A stable complex is initially formed. Within such tightly bound complex, flavodoxin rocks rapidly between different positions. The rocking of the bound flavodoxin between several different orientations gives rise to the transient complexes in fast exchange as observed in the NMR experiments. Docking simulations with two different approaches support the theory that there is no highly specific orientation in the complex, but instead one side of the flavodoxin binds the P450 with high overall affinity but with a number of different orientations. The level of functionality of each orientation is dependent on the distance between cofactors, which can vary between 8 and 25 Å, with some of the transient complexes showing distances compatible with the measured electron transfer rate constants.



## 1. Introduction

The cytochrome P450 superfamily is a group of haem-thiolate monooxygenases that have been the centre of intense research interest for many years. The P450 enzyme with the highest monooxygenase rate yet observed is CYP102A1 (P450 BM3) from *Bacillus megaterium*, with rates of up to 17,000 mol/min/mol of enzyme for arachidonic acid [1]. The protein was the first P450 system to be discovered with a fused reductase partner and this is believed to be the key to its high turnover rate. The 119 kDa protein consists of three domains: a haem containing P450 domain (P450 BMP) and a reductase (BMR) that comprises a FMN binding domain and a FAD binding one. The latter also contains the NADPH binding site [2]. The fact that P450 BM3 uses a FAD/FMN containing system sets it apart from most of the bacterial P450s, though homologues have been found in other bacteria and fungi [2], and makes it similar to the membrane bound systems found in mammals. P450 BM3 is soluble making it an attractive model system since production and handling are greatly simplified and it is possible to express the protein recombinantly, both as the complete system and as separate domains [3].

The electron transfer from the NADPH to the FAD, FMN and haem domains of the natural fusion protein has been shown to be very rapid, with a rate constant of 250 $s^{-1}$ from the FMN to haem [4]. On the other hand, the separate FAD, FMN and haem domains obtained by either proteolysis [5] or genetic engineering [6,7] were found to show very low, $1.3\pm0.3$ $s^{-1}$, electron transfer rate constants [8].

The FMN domain of P450 BM3 shares a very high sequence similarity with the family of the FMN containing flavodoxins. The possibility of electron transfer has been previously suggested when a chimera of BMP and flavodoxin from *D. vulgaris* (FLD) was immobilised on an electrode surface [9]. The improved catalytic performance of the fusion protein with respect to the wt BMP was explained with a direct participation of flavodoxin in modulating the electron transfer to the haem domain. This observation prompted the investigation of the inter-protein ET between BMP and FLD and the characterisation of the complex between the two proteins.

Transient complex formation is often found among redox proteins. Specific properties of the molecular interactions are necessary to

* Corresponding author. Division of Biomolecular Sciences, Imperial College London, SW7 2AZ London, UK. Tel.: +44 207 5945320; fax: +44 207 5945330.
*E-mail address:* g.gilardi@imperial.ac.uk (G. Gilardi).

0005-2728/$ – see front matter © 2009 Elsevier B.V. All rights reserved.
doi:10.1016/j.bbabio.2009.01.016

guarantee the formation of a complex with reasonable affinity in a very short time. For example, many of these complexes employ electrostatic attraction to increase the association rate constant [10]. By attraction and pre-orientation of the proteins upon their encounter, the number of productive collisions can be increased by several orders of magnitude, as was demonstrated by many kinetic studies on complexes of redox proteins as reviewed in [10].

Nuclear magnetic resonance is well suited to study protein–protein interactions. There are several approaches to mapping protein–protein interactions by NMR and a detailed discussion of these techniques can be found in recent reviews by Zuiderweg [11] and Prudêncio [10]. Chemical shift perturbation mapping utilises heteronuclear single quantum correlation (HSQC) spectroscopy to monitor areas of a target protein that are affected by the presence of a binding partner. As the unlabelled binding partner is titrated, the perturbations of the chemical shifts are recorded. The interactions cause environmental changes on the protein interfaces and hence affect the chemical shifts of the nuclei in this area. Flavodoxin is highly amenable to study by NMR since it is a relatively small protein. Once labelled with $^{15}N$ it displays a well-resolved HSQC spectrum that has been assigned in the oxidised form [12].

The active complex formation was therefore studied here by combining docking algorithms with NMR data in order to identify the configuration that best describes the kinetic data.

Furthermore, the aforementioned importance of electrostatic interactions in the transient complex formation was investigated by varying the ionic strength of the solution and observing the changes in the electron transfer kinetic and NMR HSQC signal.

## 2. Materials and methods

### 2.1. Electron transfer experiments

The FLD and P450 BMP were purified as previously described in [13] and [6].

The reduction of the FLD as well as the reduction and carbon monoxide binding of the P450 BMP were followed on a Hewlett-Packard 8453 diode array spectrophotometer. The FLD (6.4 μM) was photo-reduced by visible light irradiation of a 100 W tungsten lamp under steady state in the presence of the catalyst 5-deazariboflavin (5-dRf, 3.4 μM, a generous gift from Prof. S. Ghisla, University of Konstanz) and the sacrificial electron donor EDTA (0.85 mM) in 100 mM potassium phosphate buffer, pH 7.5. The semiquinone form of the FLD ($FLD_{sq}$) was formed after 20 min of irradiation, and all the experiments were performed under strict anaerobic conditions. The photo-reduction of the P450 BMP (5.1 μM) was performed under the same conditions in the absence and presence of FLD, under carbon monoxide atmosphere.

Stopped-flow kinetics experiments were performed under anaerobic conditions, using a Hi-Tech Scientific SF-61 stopped-flow spectrophotometer using a 1 cm path length cell. The experimental set up consisted of two syringes, the first containing the photo-reduced $FLD_{sq}$, the second the arachidonate-bound oxidised BMP, $(BMP\text{-}S)_{ox}$. The electron transfer between FLD and P450 BMP was measured in the presence of arachidonate in 10 mM potassium phosphate buffer, pH 7.5 and the ionic strength was adjusted by adding potassium chloride. All the buffers and proteins were made anaerobic by flushing them with argon for at least 1 h. The FLD was photoreduced in the presence of deazariboflavin and EDTA to its semiquinone form as described earlier. The solutions within the stopped-flow were allowed to equilibrate to 25 °C before mixing and the syringes were kept under carbon monoxide atmosphere. After rapid mixing of the $FLD_{sq}$ and the $(BMP\text{-}S)_{ox}$, absorbance changes were recorded at 450 nm, due to the reduction of the haem from $Fe^{3+}$ to $Fe^{2+}$ and complex formation of the reduced haem iron with the CO.

### 2.2. Protein docking

The coordinates of flavodoxin and P450 BMP were obtained from the Protein Data Bank using codes 1J8Q and 1BU7 respectively. The 1BU7 PDB file was edited to produce a monomeric structure from the crystallographic dimer. Molecular interaction simulations were performed using the docking system BiGGER [14,15], via the Chemera software suite. In a subsequent step, the putative docked structures are ranked using an interaction scoring function developed in BiGGER. The global score calculated by BiGGER is expected to select the correct complex within the first hundred solutions. In order to aid the selection process, Chemera was used to calculate the distance between the cofactors in each of the solutions and to analyse the solutions using the NMR constraints.

The coordinates of flavodoxin and P450 BMP were also submitted for docking to DOT and subsequently clustered with ClusPro [16,17] using the web interface at http://nrc.bu.edu/cluster/.

### 2.3. NMR experiments

Fully $^{15}N$ labelled flavodoxin was produced by standard nitrogen-limited procedures, using $^{15}NH_4Cl$ as the sole nitrogen source. $^{1}H–^{15}N$ HSQC spectra were recorded at 303 K on a Bruker Avance 500 DRX spectrometer operating at 11.7 T, equipped with an HCN probe and self-shielded triple axis gradients. Potassium phosphate buffer was used at 10 mM concentration and pH 7.0. Spectra were recorded in the presence of 0.5, 1.0 and 2.0 fold equivalents of P450 BMP. By adding increasing amounts of P450 BMP it is possible to identify the residues involved in the binding interface, since their chemical shift will be affected by the proximity of the cytochrome. If a cross-peak on the HSQC spectra shifts in the presence of P450 BMP, then the nucleus it corresponds to can be considered to be within 4 Å of the nucleus in P450 BMP.

## 3. Results and discussion

### 3.1. Electron transfer measurements

Electron transfer from the semiquinone form of the FLD ($FLD_{sq}$) to the oxidised arachidonate-bound P450 BMP ($(BMP\text{-}S)_{ox}$) was first studied under steady state conditions [18]. In the presence of carbon monoxide and $(BMP\text{-}S)_{ox}$, the $FLD_{sq}$ was found to donate one electron to $(BMP\text{-}S)_{ox}$ that subsequently binds the carbon monoxide giving rise to the typical absorbance peak at 450 nm, characteristic of the reduced carbon monoxide complex of $(BMP\text{-}S)_{red}$, as shown in Fig. 1A. Control experiments carried out under the same conditions, but in the absence of FLD, showed only a negligible shoulder at 450 nm (Fig. 1B).

When the complex $[FLD_{sq}–(BMP\text{-}S)_{ox}]$ is formed, electron transfer occurs to give the reduced form $(BMP\text{-}S)_{red}$. This promptly binds carbon monoxide from the saturated atmosphere, at a non-limiting rate constant of $k_{on} \sim 4\times10^6\ M^{-1}s^{-1}$ and dissociate with a $k_{off} \sim 1770\ s^{-1}$ [19–21]. Therefore, carbon monoxide binding to the P450 becomes a non-limiting step in the overall reaction as it is fast and fully reversible. The reaction mechanism can thus be simplified by considering only the complex formation and electron transfer between the flavodoxin semiquinone and the substrate bound BMP. Because the experimental conditions used did not allow obtaining true pseudo-first-order the data were fitted using the model proposed by Malatesta [22,23] for the analysis of bimolecular reactions under second-order conditions described by Eq. 1:

$$A = A_0 + A_{eq}\frac{1-e^{-k_{obs}t}}{1-\omega e^{-k_{obs}t}} \quad (1)$$

where $A$, $A_0$ and $A_{eq}$ are the absorbance at 450 nm at time $t$, 0 and at equilibrium, respectively, $k_{obs}$ is to the observed rate constant and $\omega$ a

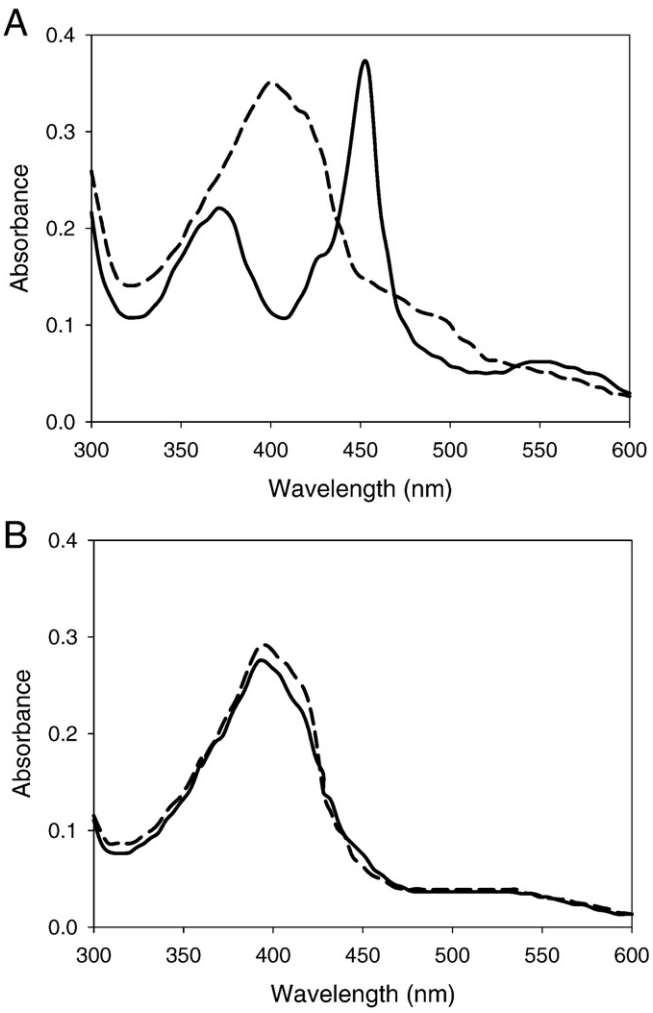


**Fig. 1.** Electron transfer between FLD and BMP under steady state conditions. The P450 BMP (5 μM) reduction and CO binding was followed in the presence (A) and absence (B) of FLD (4.9 μM) using 40 μM arachidonate, dRf, EDTA and light irradiation under anaerobic conditions. The spectrum of the substrate bound P450 BMP with the Soret peak at 397 nm (dotted line), changes upon light irradiation (solid line) only when FLD is present (A). Successful reduction by $FLD_{sq}$ and CO binding was indicated by the absorption band at 450 nm (A, solid line).

dimensionless parameter describing the deviation of the experimental conditions from pseudo-first order ($-1<\omega<1$, with $\omega=0$ when true pseudo first-order conditions apply) [23]. $\omega$ was found to be $10^{-9}$ in most of the fittings suggesting that the kinetics were following a single exponential as in true pseudo-first order conditions. The formation of the [$FLD_{sq}$–$(BMP\text{-}S)_{ox}$] complex was investigated by a concentration dependence study of the observed ET rate constants by varying the $FLD_{sq}$ from 2 to 20 μM, against a 1 μM concentration of $(BMP\text{-}S)_{ox}$.

Data fitting was performed using Eq. 2:

$$k_{obs} = \sqrt{k_{on}{}^2\left([BMP_{ox}{-}S]{-}[FLD_{sq}]\right)^2 + k_{off}^2 + 2k_{on}k_{off}\left([BMP_{ox}{-}S] + [FLD_{sq}]\right)} \quad (2)$$

where $k_{on}$ is the bimolecular rate constant for the complex formation and $k_{off}$ if the dissociation rate constant of the complex. When the experiments were carried out in 10 mM potassium phosphate at 250 mM ionic strength the calculated parameters were $1.1\times10^6\pm0.2$ $M^{-1}s^{-1}$ and $27.0\pm1.7$ $s^{-1}$ for $k_{on}$ and $k_{off}$ respectively. This suggests fast complex formation and slow dissociation with the formation of a tightly bound complex with a dissociation constant of $24.5\pm4.6$ μM. In order to study the nature of this interaction, the intermolecular electron transfer was investigated at different ionic strengths. Measurements of $k_{obs}$ were carried out at different FLD concentrations and at ionic strengths ranging from 80 mM to 400 mM. At each value of ionic strength investigated the formation of a tightly bound complex was observed. The $k_{obs}$ values were found to vary with the ionic strength following a bi-phasic dependence (Fig. 2A). Furthermore it is interesting to observe that also $k_{on}$ shows a bell shaped curve in function of the ionic strength, comprising of an ascending region at low ionic strength, a descending region at high ionic strength and a maximum value at 250 mM. Conversely, $k_{off}$ shows no dependence on the ionic strength with values oscillating between 23 and 31 $s^{-1}$ (Fig. 2A inset). This is not surprising as the increased concentration of ions will be affecting the bimolecular reaction of complex formation by screening the charges at the protein–protein interface while having very little effect on the dissociation of the complex. Consequently, also the equilibrium dissociation constant ($K_d$) calculated form the ratio of $k_{off}$ and $k_{on}$ shows dependence from the ionic strength with an opposite trend and a minimum at 250 mM (Fig. 2B).

A bi-phasic dependence of ET rate constants in function of the ionic strength has been previously observed for other redox partners, and it has been interpreted as due to a reorganisation process within the electron transfer complex [24–27]. Moreover, the flavodoxin from *Escherichia coli* has been observed to bind bovine P450C17 in an ionic strength dependent manner [28]. This dependence has often been associated with the initial formation, at low ionic strength, of a

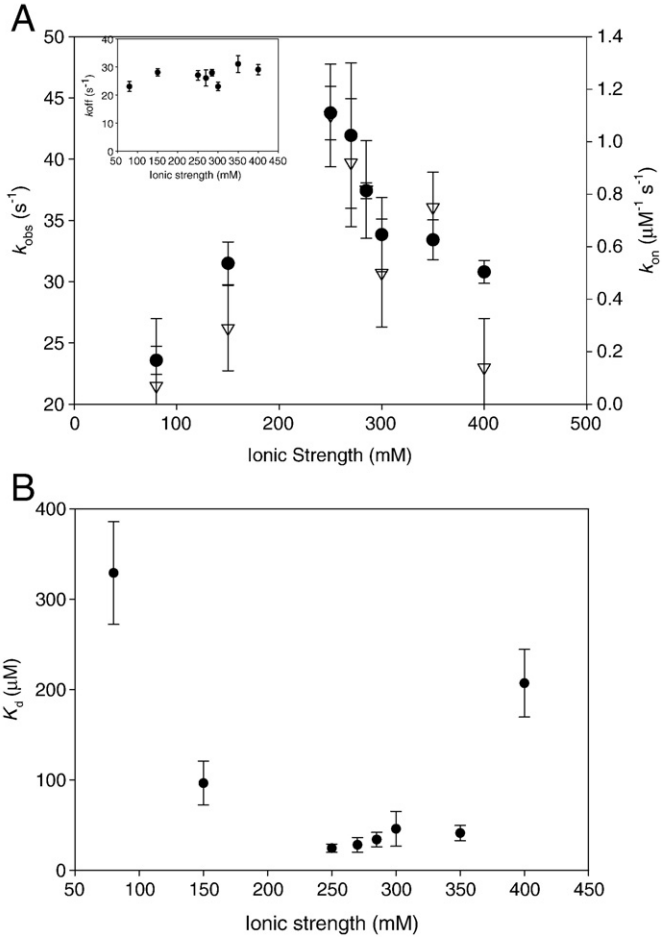


**Fig. 2.** (A) Ionic strength dependence of $k_{obs}$ ($s^{-1}$) (triangles) $k_{on}$ ($M^{-1}$ $s^{-1}$) (circles) and $k_{off}$ ($s^{-1}$) (inset) for the reaction between $FLD_{sq}$ (2–20 μM) and $(BMP\text{-}S)_{ox}$, 1 μM after mixing. The experiments were carried out at 25 °C. Parameters obtained from the fittings according to Eqs. 1 and 2. (B) Ionic strength dependence of the dissociation constant $K_d$ for the reduction of P450 BMP by the $FLD_{sq}$.

complex dominated by electrostatic interactions and characterised by a low electron transfer rate constant. Such initial complex plays a negative role in the electron transfer reaction. As the ionic strength is increased, the reorganisation of the initial complex becomes easier and the rate constant of electron transfer increases until a maximum is achieved. When the ionic strength is increased further, the strength of the electrostatic interactions weakens, leading to substantial decrease in the electron transfer rate constants.

Furthermore, it is interesting to observe that the lifetime of the complex is in the same timescale as the electron transfer time as suggested by the ratio of $k_{obs}$ and $k_{off}$ ranging from 1 to 1.6. This is a further evidence of the formation of a stable complex, as only one electron can be transferred from the FLD, the electron transfer rate becomes limited by the dissociation of the complex. In this view the changes in electron transfer rate constants measured in function of the ionic strength and the aforementioned reorganisation are probably associated to the formation of dynamic ensembles in the stable complex.

### 3.2. Docking and modelling

The electrostatic nature and in particular the importance of the charges surrounding the redox centre in the formation of ET complexes has been shown for several different systems. For example, electrostatic interactions have been shown to orient the FLD from *Clostridium pasteuranum* and *Azotobacter*, with respect to cytochrome *c* proteins that have positive charges localised around the haem [26,29–31]. Moreover, also the complex of P450cam with putidaredoxin has been shown to be electrostatically stabilised [32]. Other examples include the interaction between cytochrome *c* with either cytochrome $b_5$ [33,34], or cytochrome *c* peroxidase [35].

As the crystal structure of both proteins, flavodoxin and P450 BMP, are known, docking algorithms were used to elucidate the structural properties of the complex. The BiGGER algorithm was used with the support of the Chemera software package that was also used to view and filter the solutions. The co-ordinates of flavodoxin and P450 BMP were taken from the Protein Data Bank (1J8Q and 1BU7 respectively) and the docking was set-up using the default parameters. Two calculations were run, using each protein in turn as the target. Fig. 3 shows the top 100 solutions generated by BiGGER according to the global scoring function (for clarity the probe molecules are shown as only the cofactors). When P450 BMP is used as the target, the solutions are mainly clustered around two parts of the P450's surface with a few solutions in other positions. This would suggest two regions on P450 BMP that are suitable for flavodoxin binding, one of which is more heavily favoured by BiGGER. By contrast, when flavodoxin is used as the target the solutions are much more evenly distributed over the flavodoxin's surface. However, it does appear that the region around the FMN co-factor is not favoured by BiGGER's global scoring function, since the majority of the top 100 solutions are clustered away from this area. Of the top 100 solutions ranked by BiGGER's global scoring function, only one solution in each case has a haem to FMN distance of less than 15 Å limit set by Page et al. for a viable electron transfer [36]. However, the electron transfer rate constants measured for the P450 BMP/flavodoxin complex range from 24.2 ± 1.2 $s^{-1}$ to 44.1 ± 0.4 $s^{-1}$. We can therefore estimate a more precise value for the distance using the following equation [36]:

$$\text{Log } k_{ET} = 13 - 0.6(R - 3.6) - \left(\left(3.1(-\Delta G + \lambda)^2\right)/\lambda\right) - (\Delta G/0.06) \quad (3)$$

where $R$ is the edge to edge distance between cofactors in Å, $\Delta G$ is the driving force (in eV) and $\lambda$ is the reorganisation energy (also in eV). The value of $\Delta G$ is calculated from the difference in reduction potential between the donor and acceptor, in this case it is 85 mV or 0.085 eV (−145 mV and −230 mV for $FLD_{ox-sq}$ and BMP-S respectively); this is an endergonic reaction. The reorganisation energy can be approximated to 1.0 eV for intermolecular electron transfer as suggested in [36]. Entering these values into the above equation yield a distance between the donor and acceptor ranging from 15.92 ± 0.01 Å to 16.38 ± 0.01 Å. Using these values the number of potentially good candidates increases but no univocal solution is obtained.

The nature of the BiGGER results may be a reflection of the binding mechanism. Two-step binding processes have been proposed for other redox protein complexes, both physiological [37] and non-physiological [38]. Nevertheless, looking at the spread of potential binding sites on the flavodoxin molecule the formation of transient conformers in the stable complex might be hypothesised. Complexes may form a dynamic ensemble of conformations, governed mostly by electrostatic interactions, which is in equilibrium with the more tightly bound functional conformations [10]. The functional complexes are likely to involve hydrophobic interactions [39] and so the equilibrium position is often dependent on ionic strength. The diverse array of possible solutions generated by BiGGER may be an indication of the possible constituents of the dynamic ensemble. To facilitate the ranking of these solutions

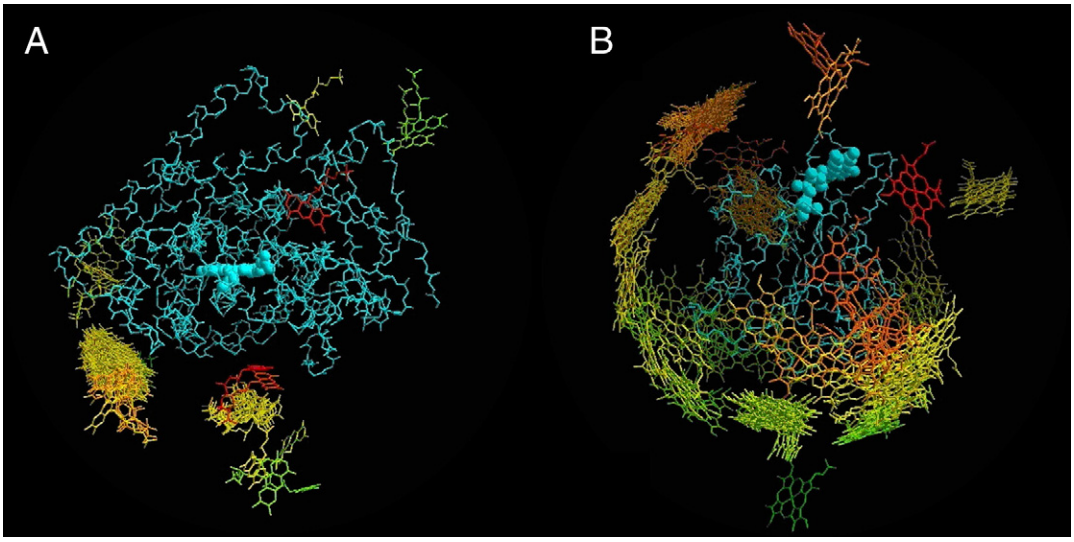


**Fig. 3.** First 100 solutions from the BiGGER calculation ranked by global score, both when using P450 BMP (A) or flavodoxin as the target (B). Solutions are displayed using only the co-factors for clarity and are coloured by their haem to FMN distance, from green (furthest) to red (closest). Target molecules are shown in blue as the α-carbon backbone only, with the co-factor displayed in spacefill.

and validate the hypothesis of the dynamic ensembles two separate approaches have been taken. Firstly a different docking algorithm with ranking capabilities was used and secondly nuclear magnetic resonance (NMR) was employed to identify the residues at the binding interface as well as to provide information on the nature of the equilibrium [10]. This approach (termed 'restrained soft-docking') has been used to determine models for the complexes of Fe-hydrogenase and cytochrome *c*553 [40], cytochrome *c*553 and ferredoxin [41] and cytochrome *c*3 with Fe-hydrogenase [42].

When the docking algorithm DOT was used and its solutions filtered with ClusPro the output consisted of 10 potential complexes. Of these 10 complexes, 8 locate the potential binding site on the BMP in a position that corresponds to one of the cluster identified by BiGGER (Fig. 4A). It is interesting to note that such binding site correspond to the area where the FMN binding portion of the reductase domain docks in the crystal structure of the complex [43]. Furthermore, considering that flavodoxin has an oblong shape with the long axis going from the FMN to the N and C terminal and analyzing the orientation of the flavodoxin in the 8 complexes, it is interesting to observe that it often binds with the long axis parallel to the BMP surface. With this orientation the flavodoxin rotates in the different complexes along the long axis exposing different residues to the BMP binding site. This is in keeping with the multiple sites observed in BiGGER when docking BMP on flavodoxin. The results of the docking with DOT were also confirmed by obtaining comparable results when using ZDOCK as alternative docking approach as well as when using the structure of the semiquinone form of flavodoxin instead of the oxidised form (data not shown).

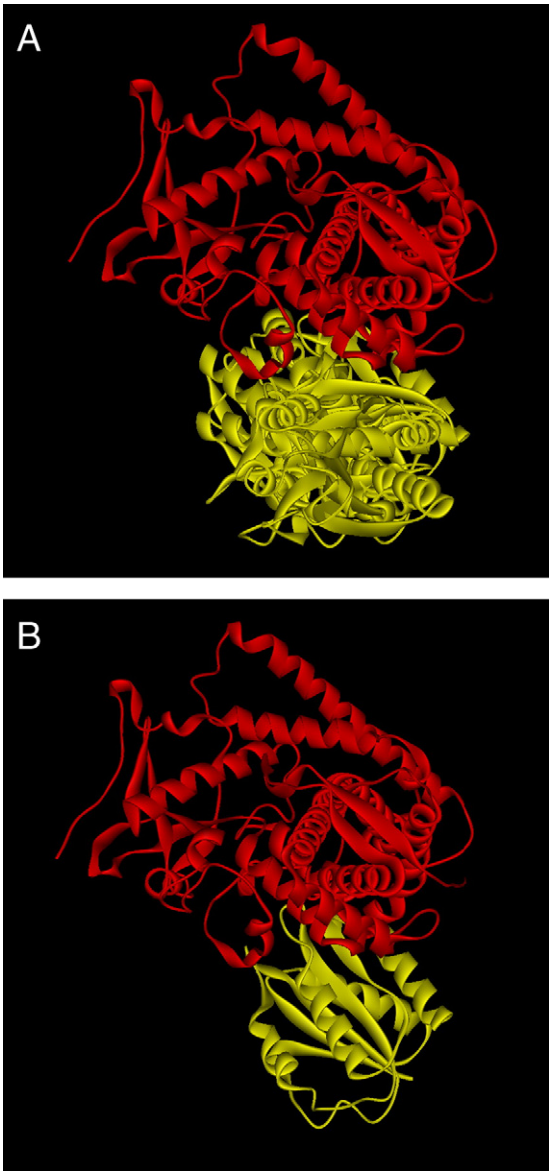


**Fig. 4.** Solutions obtained using DOT and ClusPro. Both proteins are represented as red (BMP) and yellow (FLD) solid ribbon. (A) First 8 solutions of DOT docking clustered and selected using the automatic web served ClusPro. (B) Solution number 4 showing the shortest distance between haem and FMN at 14 Å.

### 3.3. NMR measurements

The HSQC spectrum recorded for the flavodoxin alone is almost identical to that of Knauf et al. [12], with the exception of a few areas. These differences are due to the differing buffer conditions used. The following residues were not identified: threonine 11, threonine 15, glycine 61, aspartic acid 62, aspartic acid 63 and leucine 67. The peak positions of these residues have been shown to be sensitive to the conditions under which the HSQC is collected, shifting considerably when the phosphate concentration is increased to 100 mM [44]. Proline residues are not observed on a $^{15}N$–$^{1}H$ HSQC spectrum, due to the absence of a backbone N–H group. Therefore residues 73 and 130 were not observed. Fig. 5A shows a section of the flavodoxin HSQC spectra at varying P450 BMP concentrations. Since the peaks are shifting position continuously, we can conclude that the two proteins are in fast exchange, i.e. the lifetime of the complex is less than the NMR timescale. Complexes with a longer lifetime (slow exchange) will cause peaks to shift from one position to another with no intermediate points. We would expect an electron transfer complex to be short lived, since a long-lived species would unnecessarily impound the redox partners. The positions of each peak in the HSCQ spectra were recorded for different P450 BMP concentrations (0.0, 0.5, 1.0 and 2.0 fold excess with respect to flavodoxin). To help the interpretation of the results of the shift in the peak position a combined weighted average of the proton and nitrogen chemical shift changes was calculated as follows [45]:

$$\Delta\delta_{av} = \left(\left[(\Delta\delta_H)^2 + \left((\Delta\delta_N)^2/25\right)\right]/2\right)^{1/2} \quad (4)$$

where $\Delta\delta_H$ and $\Delta\delta_N$ are the changes for proton and nitrogen chemical shifts respectively. In order to elucidate the nature of the binding site, we must identify the residues that show significant change upon addition of P450 BMP. A significant change is considered to be any change above the mean of all changes plus one standard deviation. For the 2-fold excess of P450 BMP, significant changes are normalised and displayed in Fig. 5B. The backbone N–H groups of residues 9, 14, 25, 53, 64, 66, 75, 103, 132, 137, 139, 140, 142 and 145 show significant changes from the spectra of un-bound flavodoxin. The protonated N3 of the FMN also shows a significant shift, as does the "NH2 of glutamine 121. The nitrogen and hydrogen atoms of these residues can be used as constraints to filter the solutions produced by BiGGER. When all 30 residues are used as constraints, the highest number of contacts is just 13. Significantly, none of the solutions with the most contacts (13, 12 or 11 contacts) has an ideal FMN to haem distance. Also, it is impossible within each model to position all of the perturbed residues of flavodoxin in the proximity of the P450. When the perturbed residues are highlighted on the structure of flavodoxin they are found to cover a large area of its surface and may be clustered in two binding sites on opposite sides of the molecule (Fig. 6A). This, in combination with the apparent contradiction between NMR and kinetic data strongly suggests the idea of a dynamic ensemble as previously described. The association between P450 BMP and flavodoxin is strong overall, giving a low $K_d$, but flavodoxin is able to 'rock' between various orientations, each of which is short lived. In this model each residue would only be in the vicinity of the P450 for a

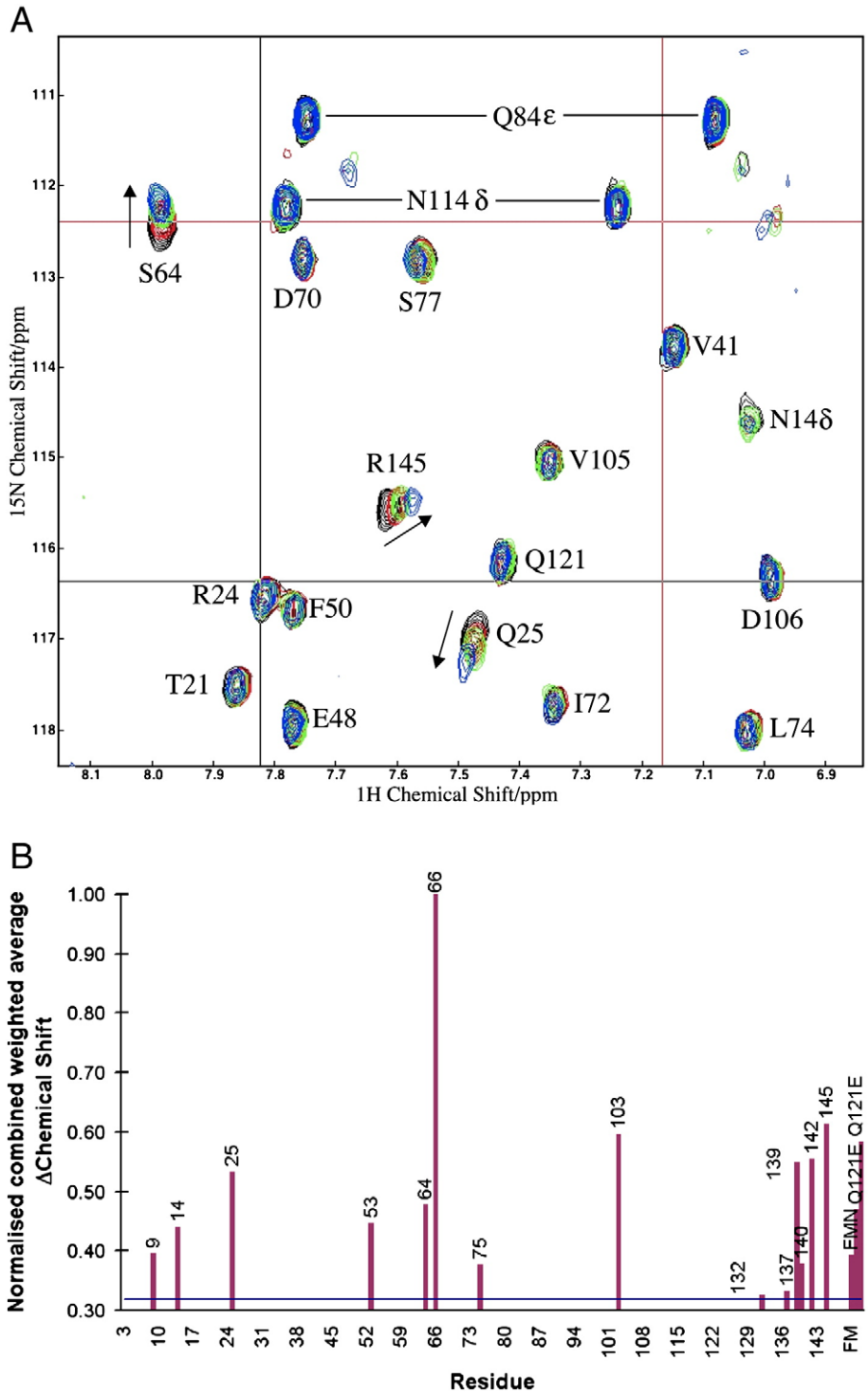


**Fig. 5.** (A) Overlay of a section of the flavodoxin HSCQ spectra at varying P450 BMP concentrations. Flavodoxin alone is shown in black with 0.5, 1.0, and 2.0 fold excess of P450 BMP shown in red, green, and blue respectively. Peaks are labelled with the residue identity and arrows indicate peak movement. (B) Changes in flavodoxin chemical shift upon addition of 2-fold P450 BMP excess. The blue line marks the level at which changes are considered to be significant and residue type and positions are labelled.

limited time, giving the impression of a short lived complex. This is also in keeping with the results of the BiGGER and DOT algorithms, which suggested that flavodoxin is able to bind P450 BMP in many orientations.

Consistently, only a fraction of the residues identified by the NMR experiments are involved at one time in each potential complex. Even when residues in the two putative binding sites were used independently only a fraction of the identified atoms are selected in the solutions with the shortest haem to FMN distance, ranging between 8.02 to 16.34 Å. This is in keeping with the hypothesis of a tight complex where the flavodoxin rapidly rocks between different orientations, some of which have ideal FMN to haem distance for electron transfer to occur. Similarly, the output of DOT-ClusPro shows 8 solutions, binding with very different orientation to the same position on the BMP (Fig. 4A), one of which (solution 4) has a FMN to haem distance of 14 Å (Fig. 4B) compatible with the measured electron transfer rate constants. Furthermore the observed complex stoichiometry for each residue in the two hypothetical binding sites might be

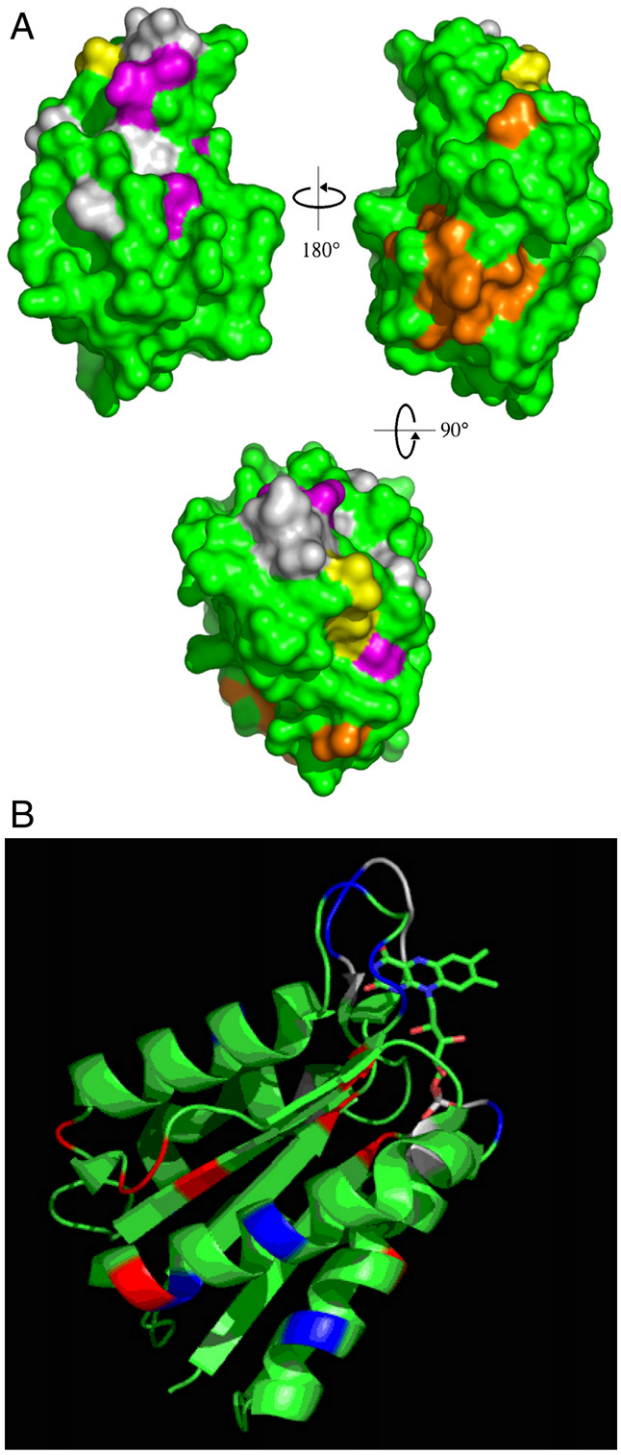


**Fig. 6.** (A) Location of perturbed residues on the 3D structure of flavodoxin. Residues that were not assigned on the HSQC spectrum are shown in white. The perturbed residues are split into two groups; those around the FMN are shown in magenta while those on the rear of the molecule are shown in orange. The FMN itself is shown in yellow. Glutamine 121 and its side chain are shown in spacefill, since only the ε NH group showed a significant perturbation. (B) Effect of ionic strength on chemical shift variation. Residues that show an increased change (>20%) upon addition of 100 mM potassium phosphate are coloured red, while those with a smaller change are shown in blue. Residues not assigned on the HSQC spectrum are shown in white. The FMN co-factor is shown in stick form.

an indication of the formation of transient complexes inside the tightly bound system.

Adding sodium chloride to the sample after the addition of P450 BMP tested the affect of ionic strength on complex formation. The ionic strength used in the HSQC experiment was initially adjusted using sodium chloride as for the kinetic experiments. The HSQC spectra collected in the presence of 100 and 200 mM sodium chloride were very noisy proving to be difficult to draw any conclusion. Instead the ionic strength was adjusted using potassium phosphate. The concentration of potassium phosphate in a solution of flavodoxin and 2.75 fold excess of P450 BMP was increased to 100 mM and a HSQC spectrum recorded. The ionic strength of this buffer is roughly equivalent to 250 mM potassium chloride, where the highest limiting electron transfer rate constant has been observed. The changes observed do not indicate that either proposed site is favoured by the increased ionic strength and instead there is a general reduction in the perturbation of surface residues in the proposed binding sites (Fig. 6B). The increase in perturbation of some internal residues is indicative of a small conformational change, which would not be unexpected given the large change in ionic strength. We would have expected the functional complex to be favoured to account for the increase in limiting electron transfer rate constant, but there is no evidence of this in the pattern of perturbed residues. It may instead be the case that the higher $k_{on}$ (Fig. 2A) and associated decrease in $K_d$ (Fig. 2B) is indicative of the formation of a tighter binding decreasing the number of 'complexes' explored in the dynamic ensemble. The increase in $K_d$ after 250 mM ionic strength is accompanied by a fall in the limiting electron transfer rate constant.

In conclusion the behaviour of the electron transfer data in relation to ionic strength implies that the complex between P450 BMP and flavodoxin is mediated by a mixture of electrostatic and hydrophobic interactions. The exact balance between the two determines the frequency with which the functional complex can occur. The apparent contradiction between the tightly bound complex observed in the electron transfer experiments and the short lived complexes observed during the NMR experiments is simply the result of the existence of two events in the complex formation prior to electron transfer. The NMR and docking data support the theory that there is no highly specific orientation in the complex; instead the flavodoxin binds the P450 with high overall affinity but rocking within a number of different orientations. The level of functionality of each orientation is dependent on the distance between cofactors, which can vary between 8 and 25 Å, with some of the transient complexes showing distances compatible with the measured electron transfer rate constant.

## References

[1] M.A. Noble, C.S. Miles, S.K. Chapman, D.A. Lysek, A.C. Mackay, G.A. Reid, R.P. Hanzlik, A.W. Munro, Roles of key active-site residues in flavocytochrome P450 BM3, Biochem. J. 339 (1999) 371–379.
[2] H.M. Girvan, T.N. Waltham, R. Neeli, H.F. Collins, K.J. McLean, N.S. Scrutton, D. Leys, A.W. Munro, Flavocytochrome P450 BM3 and the origin of CYP102 fusion species, Biochem. Soc. Trans. 34 (2006) 1173–1177.
[3] A.W. Munro, J.G. Lindsay, J.R. Coggins, S.M. Kelly, N.C. Prince, Structural and enzymological analysis of the interaction of isolated domains of cytochrome P450 BM3, FEBS Lett. 343 (1994) 70–74.
[4] J.T. Hazzard, S. Govindaraj, T.L. Poulos, G. Tollin, Electron transfer between the FMN and heme domains of cytochrome P450BM-3, J. Biol. Chem., 272 (1997) 7922–7926.
[5] L.O. Narhi, A.J. Fulco, Characterization of a catalytically self-sufficient 119,000-Dalton cytochrome P450 monooxygenase induced by barbiturates in *Bacillus megaterium*, J. Biol. Chem. 261 (1986) 7160–7169.
[6] H.Y. Li, K. Darwish, T. Poulos, Characterization of recombinant *Bacillus megaterium* cytochrome P450 BM3 and its 2 functional domains, J. Biol. Chem. 266 (1991) 11909–11914.
[7] A.W. Munro, K. Malarkey, J. McKnight, A.J. Thomson, S.M. Kelly, N.C. Price, J.G. Lindsay, J.R. Coggins, J.S. Miles, The role of tryptophan 97 of cytochrome P450 BM3 from *Bacillus megaterium* in catalytic function. Evidence against the 'covalent switching' hypothesis of P-450 electron transfer, Biochem. J. 303 (1994) 423–428.
[8] I.F. Sevrioukova, J.T. Hazzard, G. Tollin, T.L. Poulos, The FMN to heme electron transfer in cytochrome P450BM-3. Effect of chemical modification of cysteines engineered at the FMN-heme domain interaction site, J. Biol. Chem. 274 (1999) 36097–36106.
[9] A. Fantuzzi, Y.T. Meharenna, P.B. Briscoe, C. Sassone, B. Borgia, G. Gilardi, Improving catalytic properties of P450BM3 haem domain electrodes by molecular Lego, Chem. Comm. 12 (2006) 1289–1291.
[10] M. Prudêncio, M. Ubbink, Transient complexes of redox proteins: structural and dynamic details from NMR studies, J. Mol. Recognit. 17 (2004) 524–539.

[11] E.R.P. Zuiderweg, Mapping protein–protein interactions in solution by NMR spectroscopy, Biochemistry 41 (2002) 1–7.
[12] M.A. Knauf, F. Lohr, G.P. Curley, P. O, ' Farrell, S.G. Mayhew, F. Muller, H. Ruterjans, Homonuclear and heteronuclear NMR studies of oxidized *Desulfovibrio vulgaris* flavodoxin. Sequential assignments and identification of secondary structure elements, Eur. J. Biochem. 213 (1993) 167–184.
[13] G.D. Krey, E.F. Vanin, R.P. Swenson, Cloning, nucleotide sequence, and expression of the flavodoxin gene from *Desulfovibrio vulgaris* (Hildenborough), J. Biol. Chem. 263 (1988) 15436–15443.
[14] P.N. Palma, L. Krippahl, J.E. Wampler, J.J. Moura, BiGGER: a new (soft) docking algorithm for predicting protein interactions, Proteins 39 (2000) 372–384.
[15] X.J. Morelli, P. Nuno Palma, F. Guerlesquin, A.C. Rigby, A novel approach for assessing macromolecular complexes combining soft-docking calculations with NMR data, Protein Sci. 10 (2001) 2131–2137.
[16] S.R. Comeau, D.W. Gatchell, S. Vajda, C.J. Camacho, ClusPro: an automated docking and discrimination method for the prediction of protein complexes, Bioinformatics 20 (2004) 45–50.
[17] S.R. Comeau, D.W. Gatchell, S. Vajda, C.J. Camacho, ClusPro: a fully automated algorithm for protein–protein docking, Nucleic Acids Res. 32 (2004) W96–W99.
[18] V. Massey, P. Hemmerich, Light-mediated reduction of flavoproteins with flavins as catalyists, Biochemistry 17 (1978) 9–17.
[19] I.F. Sevrioukova, J.A. Peterson, Reaction of carbon monoxide and molecular oxygen with P450terp (CYP108) and P450BM-3 (CYP102), Arch. Biochem. Biophys. 317 (1995) 397–404.
[20] H.M. Girvan, D.J. Heyes, N.S. Scrutton, A.W. Munro, Laser photoreaction of NAD(P) H induces reduction of P450 BM3 heme domain on the microsecond time scale, J. Am. Chem. Soc. 129 (2007) 6647–6653.
[21] S.S. B oddupalli, B.C. Pramanik, C.A. Slaughter, R.W. Estabrook, J.A. Peterson, Fatty acid monooxygenation by P450BM-3: product identification and proposed mechanisms for the sequential hydroxylation reactions, Arch. Biochem. Biophys. 292 (1992) 20–28.
[22] F. Malatesta, The study of bimolecular reactions under non-pseudo-first order conditions, Biophys. Chem. 116 (2005) 251–256.
[23] J. Janzon, A.C. Eichorn, B. Ludwig, F. Malatesta, Electron transfer kinetics between soluble modules of *Paracoccus denitrificans* cytochrome *c*1 and its physiological redox partners, Biochim. Biophys. Acta 1777 (2008) 250–259.
[24] J.A. Watkins, M.A. Cusanovich, T.E. Meyer, G. Tollin, A parallel-plate electrostatic model for biomolecular rate constants applied to electron-transfer proteins, Protein Sci. 3 (1994) 2104–2114.
[25] Y. Feng, P.R. Swenson, Evaluation of the role of specific acidic amino acid residues in electron transfer between the flavodoxin and cytochrome *c*(3) from *Desulfovibrio vulgaris* [Hildenborough], Biochemistry 36 (1997) 13617–13628.
[26] G. Cheddar, T.E. Meyer, M.A. Cusanovich, C.D. Stout, G. Tollin, Redox protein electron-transfer mechanisms — electrostatic interactions as a determinant of reaction site in c-type cytochromes, Biochemistry 28 (1989) 6318–6322.
[27] T.E. Meyer, Z.G. Zhao, M.A. Cusanovich, G. Tollin, Transient kinetics of electron-transfer from a variety of c-type cytochromes to plastocyanin, Biochemistry 32 (1993) 4552–4559.
[28] C.M. Jenkins, M.R. Waterman, Flavodoxin and NADPH-flavodoxin reductase from *Escherichia coli* support bovine cytochrome P450c17 hydroxylase activities, J. Biol. Chem. 269 (1994) 27401–27408.
[29] R.P. Simondsen, P.C. Weber, F.R. Salemme, G. Tollin, Transient kinetics of electron-transfer reactions of flavodoxin ionic-strength dependence of semi-quinone oxidation by cytochrome-*c*, ferricyanide, and ferric ethylenediaminetetraacetic acid and computer modelling of reaction complexes, Biochemistry 21 (1982) 6366–6375.
[30] G. Cheddar, T.E. Meyer, M.A. Cusanovich, C.D. Stout, G. Tollin, Electron-transfer reactions between flavodoxin semiquinone and c-type cytochromes — comparisons between various flavodoxins, Biochemistry 25 (1986) 6502–6507.
[31] P.C. Weber, G. Tollin, Electrostatic interactions during electron-transfer reactions between c-type cytochromes and flavodoxin, J. Biol. Chem. 260 (1985) 5568–5573.
[32] A.E. Roitberg, M.J. Holden, M.P. Mayhew, I.V. Kurnikov, D.N. Beratan, V.L. Vilker, Binding and electron transfer between putidaredoxin and cytochrome P450cam. Theory and experiments, J. Am. Chem. Soc. 120 (1998) 8927–8932.
[33] J.B. Matthew, P.C. Weber, F.R. Salemme, F.M. Richards, Electrostatic orientation during electron-transfer between flavodoxin and cytochrome *c*, Nature 301 (1983) 169–171.
[34] F.R. Salemme, Hypothetical structure for an intramolecular electron-transfer complex of cytochrome *c* and cytochrome b5, J. Mol. Biol. 102 (1976) 563–568.
[35] T.L. Poulos, J.A. Kraut, Hypothetical model of the cytochrome *c* peroxidase cytochrome *c* electron transfer complex, J. Biol .Chem 255 (1980) 10322–10330.
[36] C.C. Page, C.C. Moser, X. Chen, P.L. Dutton, Natural engineering principles of electron tunnelling in biological oxidation-reduction, Nature 402 (1999) 47–52.
[37] M. Ubbink, D.S. Bendall, Complex of plastocyanin and cytochrome *c* characterized by NMR chemical shift analysis, Biochemistry 36 (1997) 6326–6335.
[38] M. Ubbink, M. Ejdebäck, B.G. Karlsson, D.S. Bendall, The structure of the complex of plastocyanin and cytochrome *f*, determined by paramagnetic NMR and restrained rigid-body molecular dynamics, Structure 6 (1998) 323–335.
[39] D.S. Bendall, Interprotein electron transfer, in: D.S. Bendall (Ed.), Protein Electron Transfer, BIOS Scientific Publishers, Oxford, UK, 1996, pp. 43–68.
[40] X. Morelli, M. Czjzek, C.E. Hatchikian, O. Bornet, J.C. Fontecilla-Camps, N.P. Palma, J.J. Moura, F. Guerlesquin, Structural model of the Fe-hydrogenase/cytochrome *c*553 complex combining transverse relaxation-optimized spectroscopy experiments and soft docking calculations, J. Biol. Chem. 275 (2000) 23204–23210.
[41] X. Morelli, A. Dolla, M. Czjzek, P.N. Palma, F. Blasco, L. Krippahl, J.J. Moura, F. Guerlesquin, Heteronuclear NMR and soft docking: an experimental approach for a structural model of the cytochrome *c*553–ferredoxin complex, Biochemistry 39 (2000) 2530–2537.
[42] L. ElAntak, X. Morelli, O. Bornet, C. Hatchikian, M. Czjzek, A. Dolla, F. Guerlesquin, The cytochrome *c*3-[Fe]–hydrogenase electron-transfer complex: structural model by NMR restrained docking, FEBS Lett. 548 (2003) 1–4.
[43] I.F. Sevrioukova, H. Li, H. Zhang, J.A. Peterson, T.L. Poulos, Structure of a cytochrome P450–redox partner electron-transfer complex, Proc. Natl. Acad. Sci. U. S. A. 96 (1999) 1863–1868.
[44] T.A. Murray, R.P. Swenson, Mechanism of flavin mononucleotide cofactor binding to the *Desulfovibrio vulgaris* flavodoxin. 1. Kinetic evidence for cooperative effects associated with the binding of inorganic phosphate and the 5′-phosphate moiety of the cofactor, Biochemistry 42 (2003) 2307–2316.
[45] S. Grzesiek, A. Bax, G.M. Clore, A.M. Gronenborn, J.S. Hu, J. Kaufman, I. Palmer, S.J. Stahl, P. Twingfield, The solution structure of HIV-1 Nef reveals an unexpected fold and permits delineation of the binding surface for the SH3 domain of Hck tyrosine protein kinase, Nat. Struct. Biol. 3 (1996) 340–345.